Plant Physiol. (1992) 100, 291–300
0032-0889/92/100/0291/10/$01.00/0

Received for publication February 4, 1992
Accepted May 4, 1992

Tissue and Subcellular Localization of Enzymes Catabolizing (*R*)-Amygdalin in Mature *Prunus serotina* Seeds[1]

Elisabeth Swain, Chun Ping Li, and Jonathan E. Poulton*

Department of Biological Sciences, University of Iowa, Iowa City, Iowa 52242

ABSTRACT

In black cherry (*Prunus serotina* Ehrh.) homogenates, (*R*)-amygdalin is catabolized to HCN, benzaldehyde, and D-glucose by the sequential action of amygdalin hydrolase, prunasin hydrolase, and mandelonitrile lyase. The tissue and subcellular localizations of these enzymes were determined within intact black cherry seeds by direct enzyme analysis, immunoblotting, and colloidal gold immunocytochemical techniques. Taken together, these procedures showed that the two β-glucosidases are restricted to protein bodies of the procambium, which ramifies throughout the cotyledons. Although amygdalin hydrolase occurred within the majority of procambial cells, prunasin hydrolase was confined to the peripheral layers of this meristematic tissue. Highest levels of mandelonitrile lyase were observed in the protein bodies of the cotyledonary parenchyma cells, with lesser amounts in the procambial cell protein bodies. The residual endosperm tissue had insignificant levels of amygdalin hydrolase, prunasin hydrolase, and mandelonitrile lyase.

(*R*)-Amygdalin [the β-gentiobioside of (*R*)-mandelonitrile] accumulates in seeds of rosaceous stone fruits (e.g. bitter almonds, peaches, cherries) (16). Upon tissue disruption, this cyanogenic diglycoside is catabolized to hydrogen cyanide via the sequential action of AH,[2] PH, and MDL (8, 9, 28). Such cyanogenesis accounts for numerous cases of acute cyanide poisoning following ingestion of these seeds by animals, including humans (5, 11). Like other cyanogenic species, rosaceous stone fruits require extensive tissue damage for initiation of large-scale cyanoglycoside catabolism. It is therefore assumed that amygdalin and its catabolic enzymes are kept separate in undamaged cherry seeds by some means of compartmentation (15). In sorghum leaves, premature cyanogenesis is prevented by compartmentation at the tissue level (7), whereas subcellular compartmentation seems more likely in other vegetative systems (2, 6, 13). How cyanogenic seed tissues, such as those found in *Prunus* species, prevent untimely HCN release remains largely unknown (19).

As part of our goal to elucidate the compartmentation of amygdalin and its catabolic enzymes in mature black cherry (*Prunus serotina* Ehrh.) seeds, polyclonal antibodies monospecific for AH, PH, and MDL, respectively, were raised and characterized (12, 27). The present study describes their use in immunolocalization of these enzymes at the tissue, cellular, and subcellular levels.

MATERIALS AND METHODS

Plant Materials

Mature black cherry (*Prunus serotina* Ehrh.) fruits were collected and processed, and their pits (endocarp enclosing seed) were stored as described previously (12).

Chemicals and Biochemicals

The following chemicals were obtained from Sigma Chemical Co.: Tween 20, 4-chloro-1-naphthol, horseradish peroxidase-conjugated GAR IgG, and 10 nm of colloidal gold-conjugated GAR IgG. The silver enhancement kit and 20 nm of colloidal gold-conjugated GAR IgG were purchased from Ted Pella Inc. (Redding, CA). LR White medium was obtained from Polysciences Inc. (Warrington, PA), nitrocellulose paper from Bio-Rad, and toluidine blue and basic fuchsin from Fisher Scientific.

Histological Examination of Black Cherry Seeds

For histological examination, seed slices (1 mm thick) were dehydrated through an ethanol-*n*-butanol series and embedded in Tissueprep wax (Fisher Scientific). Sections (20 μm) were stained with toluidine blue (14) and 0.1% (w/v) basic fuchsin and examined using an Olympus BH-2 microscope equipped with an Olympus C-35 AD camera.

TEM Immunocytochemical Localization of AH, PH, and MDL

All procedures were performed at room temperature. Using a razor blade, cotyledons were cut into thin slices (300 μm), which were further trimmed to yield 1 × 1 mm squares. Endosperm tissues were also thinly sliced (300 μm). All tissue samples were fixed for 46 h with 4% (v/v) paraformaldehyde and 2% (v/v) glutaraldehyde in PBS (50 mM potassium phosphate, pH 7.2, containing 0.2 M NaCl). After thorough washing with PBS, fixed samples were dehydrated through a graded series of ethanol (25–100%) followed by graded infiltration with LR White resin (33–100%) in ethanol. The tissues were then transferred to fresh LR White medium and incubated for 24 h with two further changes of medium. Embedding in fresh LR White medium was achieved by

[1] Supported by National Science Foundation grant DCB 89–17176.

[2] Abbreviations: AH, amygdalin hydrolase; PH, prunasin hydrolase; MDL, mandelonitrile lyase; GAR, goat anti-rabbit; IgG, immunoglobulin G; TEM, transmission electron microscope.

thermal cure in a vacuum oven at 60°C for 24 to 48 h in gelatin capsules. Ultrathin sections (0.1 μm) were cut with a DuPont diamond knife on a Sorvall Porter-Blum MT 2-B Ultramicrotome.

For immunocytochemical localization of AH, sections were collected on uncoated 200-mesh nickel grids and incubated sequentially with: (a) blocking buffer A (5% [w/v] non-fat dry milk in 10 mM Tris-HCl buffer, pH 7.4, containing 0.9% [w/v] NaCl and 0.05% [v/v] Tween 20) for 20 min, (b) affinity-purified anti-AH antiserum (ref. 12; diluted 1:5 with blocking buffer A) for 1 h; (c) blocking buffer A (10 times, 5 min each); (d) 10 nm of colloidal gold-conjugated GAR IgG (previously diluted 1:100 with blocking buffer A) for 1 h; and (e) distilled water.

For PH localization, ultrathin sections were collected on 300-mesh nickel grids and sequentially exposed to: (a) blocking buffer B (20 mM Tris-HCl, pH 7.4, containing 0.2 M NaCl and 10% heat-inactivated, normal goat serum) for 1 h; (b) affinity-purified anti-PH antiserum (ref. 12; containing 10% [w/v] goat serum, 1% [w/v] BSA, and 0.05% [v/v] Tween 20) for 3 to 4 h; (c) blocking buffer B (5 times, 5 min each); (d) 20 nm of colloidal gold-conjugated GAR IgG (previously diluted 1:10 with blocking buffer B) for 2 to 3 h; and (e) distilled water.

For MDL localization, grids were exposed to: (a) blocking buffer A for 1 h; (b) anti-MDL antiserum (ref. 27: diluted 1:5 with blocking buffer A) for 4 h; (c) blocking buffer A (5 times, 5 min each); (d) 20 nm colloidal gold-conjugated GAR IgG (diluted 1:20 with blocking buffer A) for 3 h; and (e) distilled water.

Grids were examined using an Hitachi H-7000 electron microscope at 50 kV. The specificity of labeling was determined on the basis of the following control treatments: (a) sections were incubated with preimmune sera instead of affinity-purified antisera, (b) sections were incubated with secondary antibody without prior exposure to a primary antibody, and (c) sections were incubated with affinity-purified antisera previously exposed to nitrocellulose paper preloaded with either AH, PH, or MDL (1–2 mg homogeneous enzyme [12, 27] per ml of respective antiserum). The third control was evaluated against each immune serum, which had been similarly incubated with nitrocellulose paper to which PBS rather than enzyme had been applied. Comparisons between immune and control sera treatments were made under double-blind conditions.

Light Microscope-Level Immunolocalization of AH, PH, and MDL

Sections (0.5–1.0 μm thick), obtained as described above, were collected on glass microscope slides and baked at 60°C for 2 to 12 h to ensure secure attachment. Exposure to primary and secondary antisera was undertaken essentially as described above for TEM localization of AH, except that all secondary antisera were diluted 1:10 with blocking buffer A before use. However, after the sections were washed for the last time with distilled water, they were treated with a silver enhancement kit (Ted Pella Inc.) according to the manufacturer's instructions, thereby enhancing the colloidal gold label. Sections were poststained with 0.1% (w/v) basic fuchsin for 2 s, washed extensively with distilled water, and dried at 25°C After mounting the section in Permount (Fisher Scientific), the distribution of colloidal silver was recorded using an Olympus BH-2 microscope equipped with an Olympus C-35 AD camera. The same immunocytochemical controls were used here as described above for TEM.

Western Immunoblotting Analysis of Extracts from Various Seed Parts

Cotyledons, endosperm, and embryonic axes were separated and individually homogenized at 4°C in a mortar with 0.5% (w/v) polyvinylpolypyrrolidone, 5% (w/v) sand, and 0.1 M histidine-HCl buffer, pH 6.0. Prior to immunoblotting analysis, homogenates were centrifuged for 5 min in a Beckman Microfuge, and supernatants were diluted to contain equal protein concentrations as determined by the Bradford (1) procedure Proteins were subjected to SDS-PAGE on 10% gels (10), electroblotted to nitrocellulose membranes using a Bio-Rad Trans-Blot apparatus (25), and challenged with monospecific polyclonal ant bodies (12, 27). Anti-AH, anti-PH, and anti-MDL antisera were diluted 1:500, 1:500, and 1:750, respectively, before use. Immune complexes were visualized using horseradish peroxidase-conjugated GAR IgG (diluted 1:3000) as secondary antibody (25).

Tissue Localization of AH by Tissue Printing

Nitrocellulose paper was prewetted with 10 mM Tris-HCl, pH 7.4, containing 0.9% (w/v) NaCl and blotted dry on Whatman 3MM paper. Black cherry seeds were halved (transverse section) with a razor blade, and their cut surfaces were applied to the nitrocellulose with slight finger pressure for 20 s (22). Tissue blots were then immunoanalyzed as described previously (25).

Protein Determination and Enzyme Assays

Protein was determined by the Bradford procedure (1) using a Bio-Rad protein assay kit with BSA serving as standard. AH, PH, and MDL activities were assayed as previously described (9, 28).

RESULTS AND DISCUSSION

The Role of Compartmentation in Preventing Cyanogenesis

Because tissue disruption is required for large-scale HCN release by cyanogenic plants, it seems probable that the cyanogenic glycosides (or, in some species, cyanolipids) and their respective catabolic enzymes have different tissue or subcellular localizations in undamaged organs. Recent studies involving a wide range of plant species and organs have not yet revealed a common compartmentation strategy for avoiding premature cyanogenesis (15). In leaves of 6-d-old light-grown sorghum seedlings, compartmentation occurs at the tissue level (7). The cyanoglucoside (*S*)-dhurrin is located in vacuoles of epidermal cells, whereas its β-glucosidase and α-hydroxynitrile lyase exist almost exclusively in the underlying mesophyll cells (18, 26). For other cyanogenic species (2, 6,

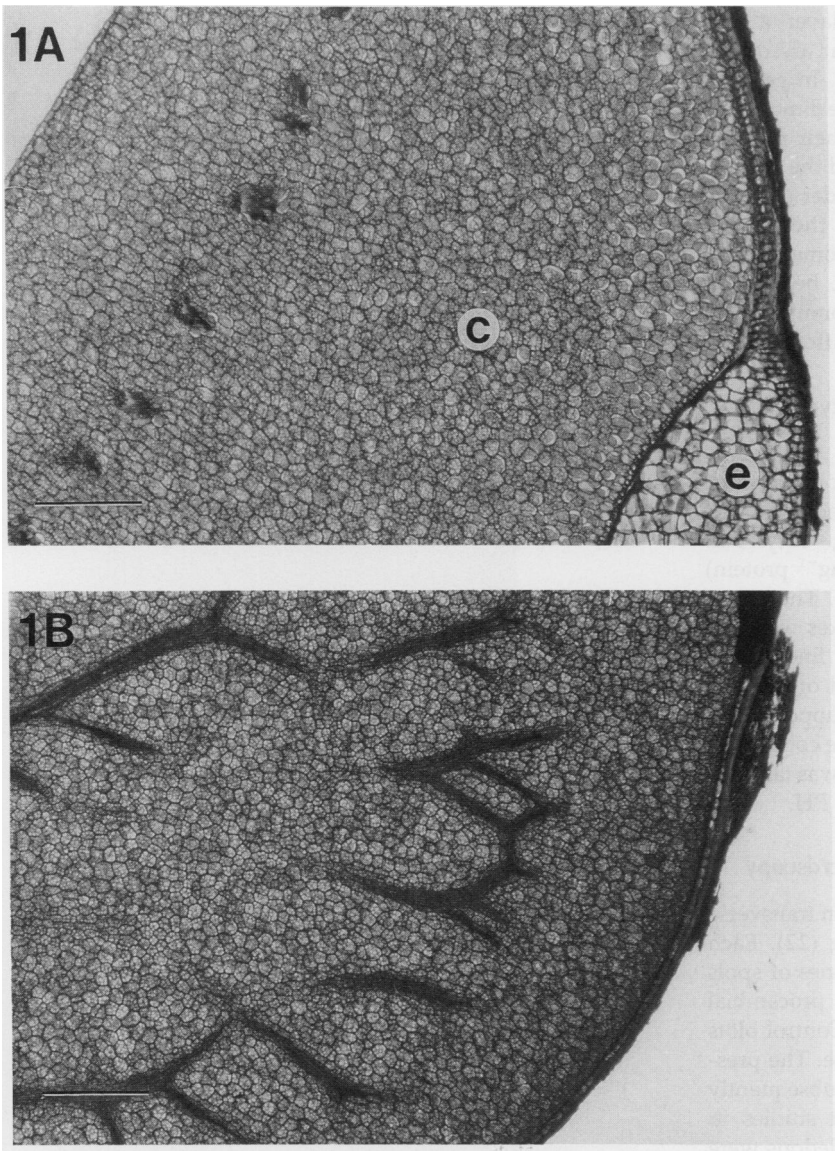

Figure 1. General anatomy of *P. serotina* seeds. A, Paraffin section through cotyledon (c) and endosperm (e) tissues showing procambial strands in transverse view. B, Section through cotyledon showing procambium in longitudinal view. Scale bar equals 200 μm.

13, 19), localization data have been interpreted largely in terms of compartmentation at the subcellular level, although in most cases, both components of the "cyanide bomb" have not been unequivocally localized within the same cells. For example, although linamarin and linamarase show similar radial gradients in tissue blocks cut from cassava root cross-sections (6), this observation does not of itself preclude tissue level compartmentation because the exact locations of both glycoside and glycosidase within such blocks remain undetermined.

Our laboratory has for several years utilized *P. serotina* as an experimental system to focus upon temporal and spatial regulation of cyanogenesis in rosaceous stone fruits. In recent studies (25), we monitored biochemical changes related to cyanogenesis that occur during fruit maturation. Seeds first became cyanogenic as the developing cotyledons rapidly accumulated both amygdalin and its catabolic enzymes AH, PH, and MDL. Although the pericarp also accumulated amygdalin, it lacked these enzymes and, thus, remained acyanogenic throughout all developmental stages. The present studies describe ongoing efforts to determine the tissue, cellular, and subcellular localizations of amygdalin and its degradative enzymes in order to reveal how premature cyanogenesis is prevented in intact black cherry seeds.

Anatomy and Histology of Black Cherry Seeds

In mature *P. serotina* fruits, the majority of the seed cavity is filled by two fleshy cotyledons that enclasp a diminutive embryonic axis (25). The residual endosperm tissue is restricted to two thin strips of cells adhering to the surrounding testa. Cotyledonary parenchyma cells are roughly isodiametric (approximately 12 μm diameter) and contain numerous oil and protein bodies. Ramifying throughout this storage tissue is a complex reticulate system of procambial strands (Fig. 1, A and B), which radiate outwards from the embryonic

axis. Each strand is circumscribed by a distinct layer of cells (henceforth designated bundle sheath cells) that are differentially stained by toluidine blue (see Fig. 4D). In general, the procambium consists of elongated cells whose dimensions and appearance vary somewhat according to their position within the procambial strand. Those cells toward the periphery of each strand are typically shorter and wider (average dimensions: 25 μm long × 8 μm wide) than those lying internally (average dimensions: 100 × 3 μm). In some strands, the latter include small groups of cells, which, because of their extremely elongated nature and lack of prominent protein bodies, are regarded as being more highly differentiated.

Localization of AH and PH within Seeds by Enzyme Analysis and Immunoblotting

Prior to immunocytochemical studies, the occurrence of AH and PH in cell-free extracts from various seed parts was probed by enzyme assays and immunoblotting. Cotyledon extracts had high AH (6.5 μmol glucose/min mg^{-1} protein) and PH (4.5 μmol/min mg^{-1} protein) activities. The corresponding values for extracts from embryonic axes were 9.9 and 2.8 μmol/min mg^{-1} protein, respectively. Endosperm extracts lacked both activities. This pronounced organ-specific distribution of these β-glycosidases was supported by immunoblotting studies (Fig. 2, A and B). Because cotyledons constitute the majority of the embryo, this organ was targeted for immunocytochemical localization of AH and PH.

Immunolocalization of AH and PH by Light Microscopy

The distribution of AH within cotyledons (cut in transverse section) was initially probed by tissue printing (22). Each cotyledon yielded a blot consisting of a linear series of spots corresponding exactly with the arrangement of procambial strands shown in Figure 1A (data not shown). Control blots challenged with preimmune serum were negative. The presence of AH within cells of the procambium was subsequently confirmed by silver-enhancement immunogold studies in which thin sections of LR White-embedded cotyledons were challenged with monospecific anti-AH antibodies (12). Whereas immunolabel was conspicuously absent from cotyledonary storage parenchyma and bundle sheath cells, cells of the procambium were intensely labeled, specifically in their protein bodies (Fig. 3, A and B). Their lipid bodies and cell walls were apparently devoid of AH, because they remained unlabeled. Noteworthy, however, is the observation that although the majority of procambial cells were heavily labeled, the small groups of more highly differentiated cells located in some procambial strands clearly lacked immunolabel (Fig. 3, A and B). Control tissue sections, which were exposed to preimmune serum (Fig. 4, A and B) or to antisera previously exposed to immobilized AH (data not shown), lacked immunolabel.

Tissue sections challenged with affinity-purified (12) anti-PH antisera showed that PH was restricted solely to protein bodies of the peripheral cells of the procambium (Fig. 3, C and D). Comparison with serial sections probed with anti-AH antisera (Fig. 3, A and B) indicates that, in these particular cells, AH and PH reside within the same protein bodies. By

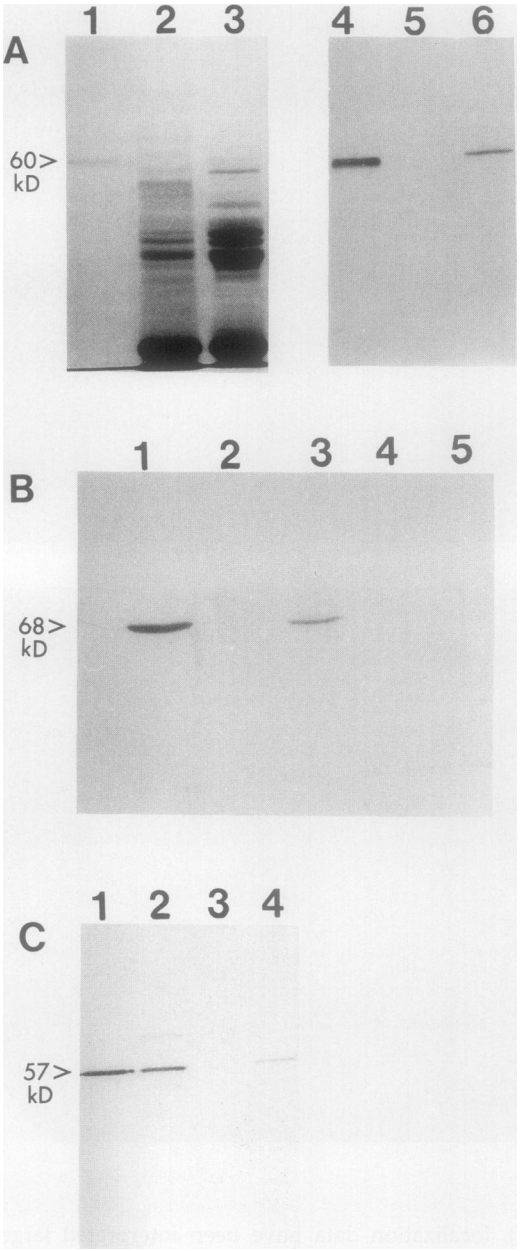

Figure 2. Western immunoblot analysis of AH, PH, and MDL levels within various seed parts. A, Homogeneous AH (0.1 μg; lanes 1 and 4) and aliquots (15 μg total protein) of proteins extracted from endosperm (lanes 2 and 5) and cotyledons (lanes 3 and 6) were subjected to SDS-PAGE. Proteins were either stained by Brilliant Blue G-Colloidal (lanes 1–3) or electroblotted onto nitrocellulose and immunodecorated with affinity purified anti-AH antiserum (lanes 4–6). B, Aliquots (7.5 μg total protein) of proteins extracted from cotyledons (lane 1), embryonic axis (lane 3), and endosperm (lane 5) were subjected to SDS-PAGE, electroblotted onto nitrocellulose, and immunodecorated with affinity-purified anti-PH antiserum. Lanes 2 and 4 were unused. C, Aliquots (6.1 μg total protein) of proteins extracted from cotyledons (lane 1), embryonic axis (lane 2), and endosperm (lane 4) were subjected to SDS-PAGE and electroblotting before being immunodecorated with anti-MDL antiserum. Lane 3 was unused.

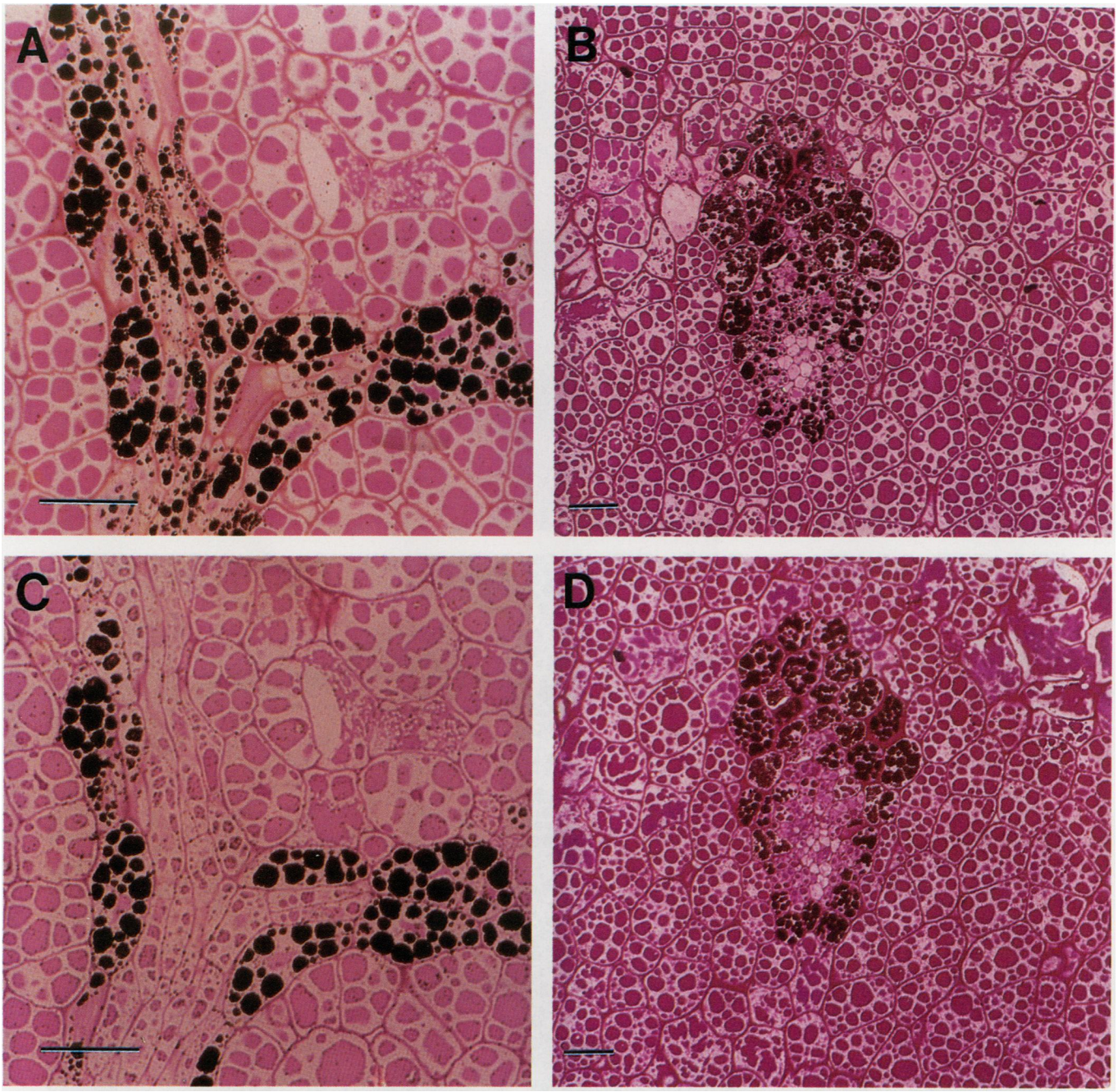

Figure 3. Tissue localization of AH and PH by silver-enhanced immunogold labeling. Serial longitudinal (A and C) and transverse (B and D) sections of cotyledons embedded in LR White resin were challenged with either anti-AH (A and B) or anti-PH (C and D) antisera. Antisera were diluted 1:40 and 1:10, respectively, before use. Poststaining was undertaken with basic fuchsin. Immunogold-labeled antigens appear as black areas after silver enhancement. Control sections exposed to preimmune serum are shown in Figure 4 (A and B). Scale bar equals 25 μm.

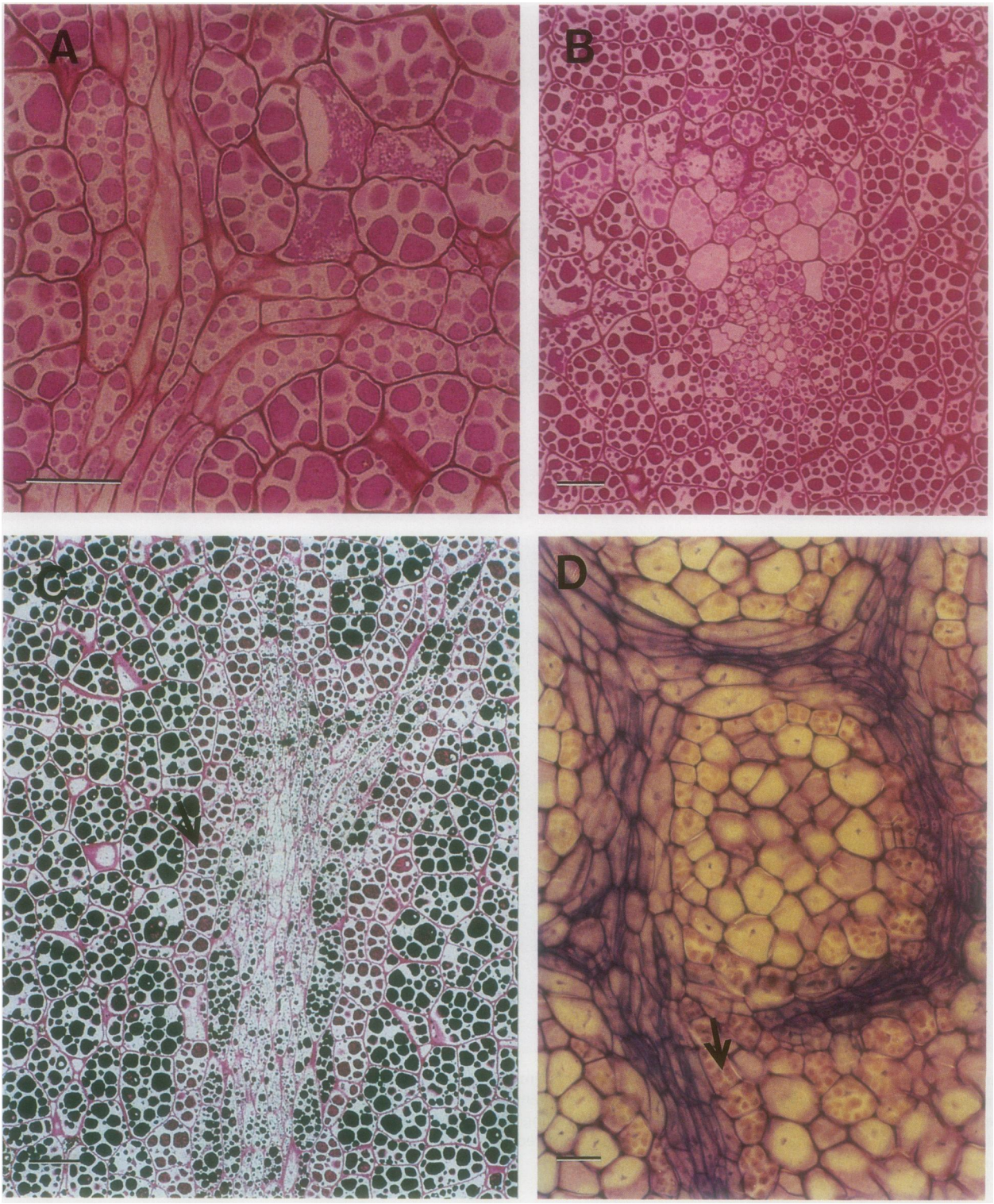

Figure 4. Tissue localization of MDL by silver-enhanced immunogold labeling. Longitudinal (A and C) and transverse (B) sections of cotyledons embedded in LR White resin were challenged with preimmune serum (A and B) or anti-MDL antiserum (C). Antisera were diluted 1:4 before use. Poststaining was undertaken with basic fuchsin. Immunogold-labeled antigen appears as black areas after silver enhancement. MDL, present in both cotyledon parenchyma and procambium, is absent from bundle sheath cells (C). Surrounding each procambial strand, the latter cells constitute a distinct layer made visible by toluidine blue staining of paraffin sections (D). The bundle sheath is indicated in panels C and D by arrows. Scale bar equals 25 μm.

contrast, PH was absent from the more internal procambial cells, including those housing AH, and from the bundle sheath and cotyledonary storage parenchyma. Control sections exposed to preimmune serum (Fig. 4, A and B) or to immune serum pre-exposed to immobilized PH (data not shown) were also unlabeled.

Confirmation of Subcellular Localizations of AH and PH by TEM

Immunogold labeling at the TEM level confirmed the subcellular localizations of AH and PH within specific cells of the procambium. In sections challenged with anti-AH antibodies, gold label was abundantly and evenly distributed throughout the matrix of protein bodies of all cells of the procambium except for those groups of more highly differentiated cells previously distinguished by light microscopy (Fig. 5A). Very few gold particles were seen over the lipid bodies, nuclei, or cell walls. Likewise, immunolabel was absent from bundle sheath and cotyledonary storage parenchyma (Fig. 5C) cells. In control experiments, in which anti-AH antisera were replaced by preimmune serum (Fig. 5B) or antisera pre-exposed to immobilized AH (data not shown), cotyledon sections exhibited extremely low backgrounds. Similarly, sections incubated with secondary antibodies alone lacked gold label.

Confirming the light microscope data, cotyledon sections challenged with anti-PH antisera showed TEM immunolabeling solely in the peripheral procambial cells. Restricted to the protein bodies, labeling was of uniform density throughout the matrix (Fig. 5D). Control sections lacked significant immunolabel (Fig. 5E).

LR White-embedded endosperm sections were also examined using immunogold staining. Supporting the immunoblotting data (Fig. 2), no gold labeling was observed using anti-AH antisera or anti-PH antisera as primary antibodies (data not shown).

Reassessment of MDL Localization

Previous attempts (27) at immunocytochemical localization of MDL in *P. serotina* seeds employed Spurr's epoxy resin (23) for embedding. Curiously, immunolabeling was observed in protein bodies and cell walls of both cotyledon and endosperm cells. Two factors have subsequently encouraged us to reassess the validity of these data: (a) the reported shortcomings of Spurr's resin for immunocytochemistry compared to acrylic resins (e.g. refs. 3, 17), and (b) enzyme analysis and immunoblotting (Fig. 2C) of endosperm tissue strips failed to detect any greater MDL levels than might easily be explained by contamination by adhering cotyledon (or testa) cells. The immunolocalization of MDL was therefore repeated here using LR White-embedded seed tissues. Silver enhancement studies showed that MDL was located primarily in cotyledonary parenchyma cells and, to a lesser extent, in cells of the procambium (Fig. 4C). In both tissues, immunolabel was restricted to the protein bodies and was not visible in the cell walls. The bundle sheath cells, which lacked AH and PH (Fig. 3, A–D), were also conspicuously free of label. This tissue and subcellular distribution of MDL was confirmed by TEM immunogold studies (Fig. 6, A–C). Unlike data previously obtained from Spurr's-embedded material (27), the cell walls of all tissues appeared essentially free of immunolabel. Furthermore, endosperm sections remained unlabeled (data not shown), a finding consistent with the immunoblotting data (Fig. 2C).

CONCLUSION

The localization of enzymes catabolizing cyanogenic glycosides is still in its infancy. Linamarase, which catalyzes the hydrolysis of the aliphatic cyanogenic glycosides linamarin and lotaustralin, has an apoplastic location in *Hevea brasiliensis* endosperm (19) and in leaves of *Trifolium repens* (4), *Phaseolus lunatus* (2), and cassava (13). The sorghum dhurrinase, however, is associated with plastids (26). Hydroxynitrile lyases are believed to be intracellular enzymes, although their precise subcellular location is not known with certainty (2, 19, 26). In this study, immunocytochemical techniques at both light and TEM levels have unequivocally localized AH and PH to protein bodies of selected procambial cells in black cherry seeds. MDL, whose levels increase concomitantly with those of AH and PH during Phases II and III of cherry fruit development (25), shows a distinct tissue localization pattern, being present in both the cotyledonary storage parenchyma and the procambium, but absent from the bundle sheath. Given the prevalence of MDL in mature seeds (approximately 5–10% of soluble proteins) and its probable location with amandins (24) in cotyledonary protein bodies, this enzyme might serve as a storage protein in addition to its primary role in cyanogenesis. With localization of AH, PH, and MDL now complete, we are currently attempting the tissue and subcellular localization of amygdalin in order to reveal which mode of compartmentation allows undamaged black cherry seeds to avoid suicidal cyanogenesis. The absence of AH and PH in bundle sheaths and cotyledon parenchyma renders these tissues attractive potential locations for amygdalin. However, the coexistence of amygdalin, AH, and PH in cells of the procambium cannot yet be ruled out. Should the latter be true, cyanogenesis would probably be prevented by some means of subcellular compartmentation.

In recent years, evidence supporting an additional role for cyanogenic glycosides and cyanolipids as storage compounds for reduced nitrogen has been mounting (20, 21). The best documented case involves the mobilization of linamarin (as the diglycoside linustatin) from *H. brasiliensis* endosperm cells to the developing shoot system (21). After catabolism within the leaves to HCN, its nitrogen is reassimilated into asparagine by action of β-cyanoalanine synthase and associated enzymes. It is tempting to speculate that the exclusive location of AH and PH in procambial cells of *P. serotina* seeds might indicate a role for these enzymes in a similar process in black cherry. Amygdalin might pass to the differentiating vascular tissue upon germination, be degraded there by AH (and perhaps PH), and its reduced nitrogen be translocated to growing regions either as prunasin or, after reassimilation, as β-cyanoalanine or asparagine. β-Cyanoalanine synthase, which exists at high levels (3 μmol HCN assimilated/min mg^{-1} protein) in mature and germinating black cherry seeds, has been purified over 400-fold from this source (unpub-

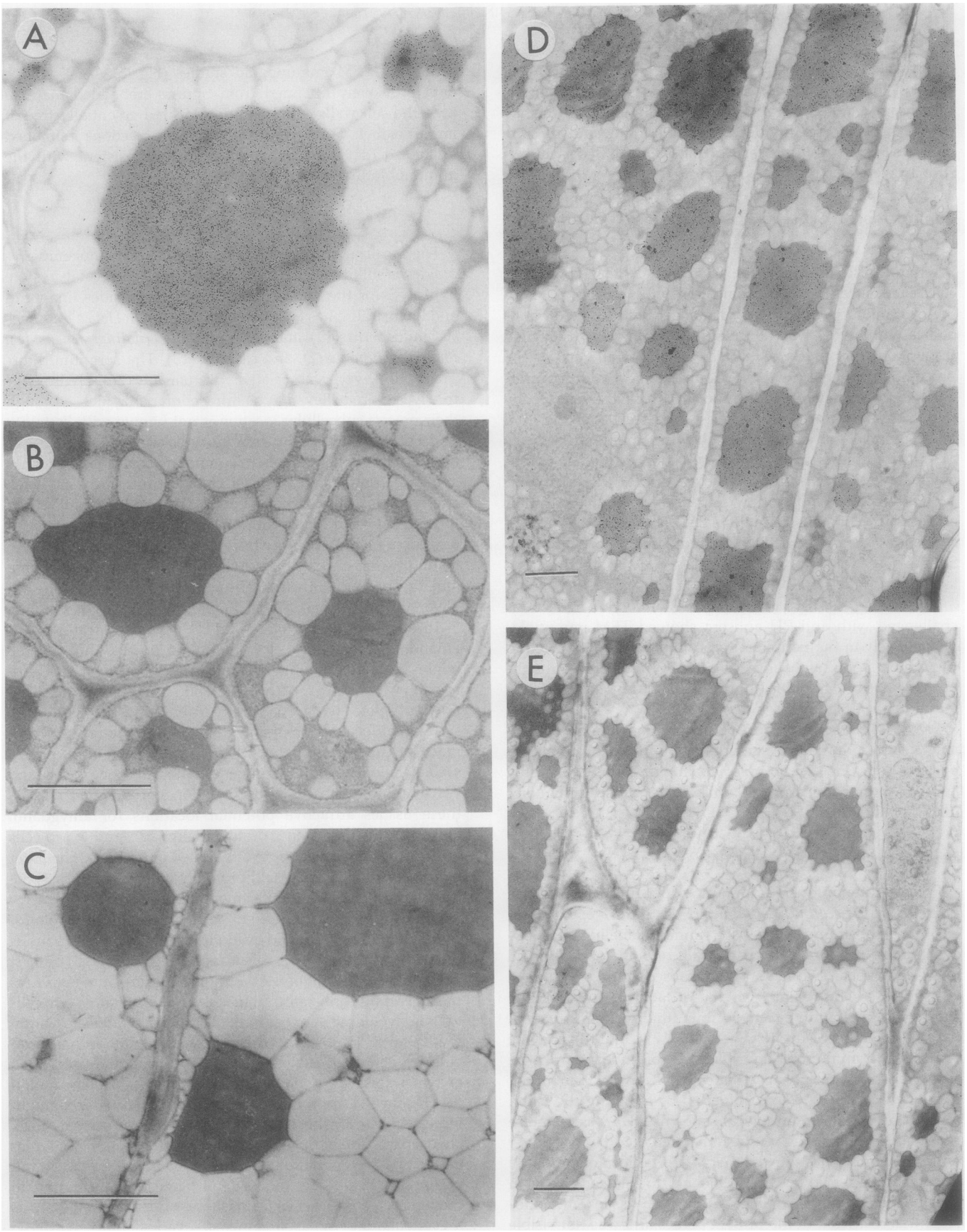

Figure 5. Immunogold TEM localization of AH and PH in black cherry seeds. Thin sections of procambial (A, B, D, and E) or cotyledon parenchyma cells (C) were exposed to the following primary antisera: A and C, affinity-purified rabbit anti-AH; D, affinity-purified rabbit anti-PH; B and E, preimmune serum. Bound antibodies were visualized using colloidal gold-conjugated GAR IgG. The elongated nature of procambial cells is illustrated by the transverse (A and B) and longitudinal sections (D and E) of these cells. Scale bar equals 2 μm.

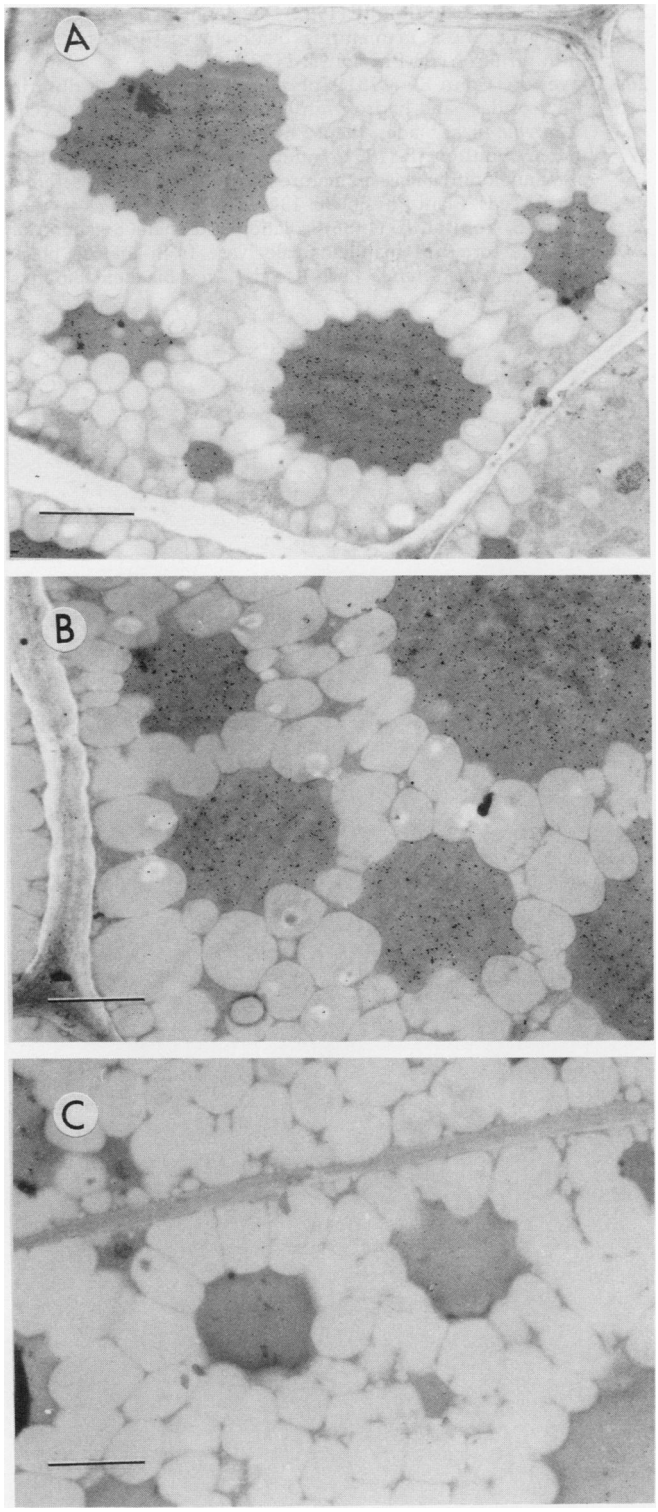

Figure 6. Immunogold TEM localization of MDL in black cherry seeds. Procambial (A) and cotyledonary parenchyma (B) cells were treated with anti-MDL antiserum. Bound MDL antibodies were localized by GAR immunogold IgG. As a control, cotyledonary parenchyma cells (C) were also exposed to preimmune serum before treatment with immunogold IgG. Scale bar equals 2 μm.

lished data). We intend to determine the location of this cyanide detoxification enzyme relative to those of AH, PH, and MDL by immunocytochemistry.

ACKNOWLEDGMENTS

The authors wish to thank Mark B. Woerner for assistance with photography and Linda C. Anthony for help in manuscript preparation.

LITERATURE CITED

1. **Bradford M** (1976) A rapid and sensitive method for the quantitation of microgram quantities of protein utilizing the principle of protein-dye binding. Anal Biochem **72:** 248–254
2. **Frehner M, Conn EE** (1987) The linamarin β-glucosidase in Costa Rican wild lima beans (*Phaseolus lunatus* L.) is apoplastic. Plant Physiol **84:** 1296–1300
3. **Herman EM** (1988) Immunocytochemical localization of macromolecules with the electron microscope. Annu Rev Plant Physiol **39:** 139–155
4. **Kakes P** (1985) Linamarase and other β-glucosidases are present in the cell walls of *Trifolium repens* L. leaves. Planta **66:** 156–160
5. **Kingsbury JM** (1964) Poisonous plants of the United States and Canada. Prentice-Hall Inc., Englewood Cliffs, NJ, pp 365–370
6. **Kojima M, Iwatsuki N, Data ES, Villegas CDV, Uritani I** (1983) Changes in cyanide content and linamarase activity in wounded cassava roots. Plant Physiol **72:** 186–189
7. **Kojima M, Poulton JE, Thayer SS, Conn EE** (1979) Tissue distributions of dhurrin and of enzymes involved in its metabolism in leaves of *Sorghum bicolor*. Plant Physiol **63:** 1022–1028
8. **Kuroki GW, Poulton JE** (1986) Comparison of kinetic and molecular properties of two forms of amygdalin hydrolase from black cherry (*Prunus serotina* Ehrh.) seeds. Arch Biochem Biophys **247:** 433–439
9. **Kuroki GW, Poulton JE** (1987) Isolation and characterization of multiple forms of prunasin hydrolase from black cherry (*Prunus serotina* Ehrh.) seeds. Arch Biochem Biophys **255:** 19–26
10. **Laemmli UK** (1970) Cleavage of structural proteins during the assembly of the head of bacteriophage T_4. Nature **227:** 680–685
11. **Lewis J** (1977) Laetrile. West J Med **127:** 55–62
12. **Li CP, Swain L, Poulton JE** (1992) *Prunus serotina* amygdalin hydrolase, and prunasin hydrolase. Purification, N-terminal sequencing and antibody production. Plant Physiol **100:** 282–290
13. **Mkpong OE, Yan H, Chism G, Sayre RT** (1990) Purification, characterization, and localization of linamarase in cassava. Plant Physiol **93:** 176–181
14. **O'Brien TP, Feder N, McCully ME** (1964) Polychromatic staining of plant cell walls by toluidine blue O. Protoplasma **59:** 367–373
15. **Poulton JE** (1988) Localization and catabolism of cyanogenic glycosides. *In* D Evered, S Harnett, eds, Cyanide Compounds in Biology. Ciba Foundation Symposium No. 140, John Wiley & Sons, Chichester, UK, pp 67–91
16. **Poulton JE** (1989) Toxic compounds in plant foodstuffs: cyanogens. *In* JE Kinsella, WG Soucie, eds, Food Proteins. The American Oil Chemists' Society, Champaign, IL, pp 381–401
17. **Robinson DG, Ehlers U, Herken R, Herrmann B, Mayer F, Schurmann FW** (1987) Methods of Preparation for Electron Microscopy. Springer-Verlag, Berlin, pp 44–52
18. **Saunders JA, Conn EE** (1978) Presence of the cyanogenic glucoside dhurrin in isolated vacuoles from *Sorghum*. Plant Physiol **61:** 154–157
19. **Selmar D, Frehner M, Conn EE** (1989) Purification and properties of endosperm protoplasts of *Hevea brasiliensis* L. J Plant Physiol **135:** 105–109

20. **Selmar D, Grocholewski S, Seigler DS** (1990) Cyanogenic lipids. Utilization during seedling development of *Ungnadia speciosa*. Plant Physiol **93:** 631–636
21. **Selmar D, Lieberei R, Biehl B** (1988) Mobilization and utilization of cyanogenic glycosides. The linustatin pathway. Plant Physiol **86:** 711–716
22. **Spruce J, Mayer AM, Osborne DJ** (1987) A simple histochemical method for locating enzymes in plant tissue using nitrocellulose. Phytochemistry **26:** 2901–2903
23. **Spurr AR** (1969) A low-viscosity epoxy resin embedding medium for electron microscopy. J Ultrastruct Res **26:** 31–43
24. **Steenkamp DJ, Joubert FJ** (1967) The microheterogeneity of amandin. J S Afr Chem Inst **20:** 81–91
25. **Swain E, Li CP, Poulton JE** (1992) Development of the potential for cyanogenesis in maturing black cherry (*Prunus serotina* Ehrh.) fruits. Plant Physiol **98:** 1423–1428
26. **Thayer SS, Conn EE** (1981) Subcellular localization of dhurrin β-glucosidase and hydroxynitrile lyase in the mesophyll cells of *Sorghum* leaf blades. Plant Physiol **67:** 617–622
27. **Wu H-C, Poulton JE** (1991) Immunocytochemical localization of mandelonitrile lyase in mature black cherry (*Prunus serotina* Ehrh) seeds. Plant Physiol **96:** 1329–1337
28. **Yemm RS, Poulton JE** (1986) Isolation and characterization of multiple forms of mandelonitrile lyase from mature black cherry (*Prunus serotina* Ehrh.) seeds. Arch Biochem Biophys **247:** 440–445